doi:10.1016/j.jmb.2004.08.060 J. Mol. Biol. (2004) 343, 671–684

JMB

Available online at www.sciencedirect.com

SCIENCE DIRECT®

ELSEVIER

Structures of Unliganded and Inhibitor Complexes of W168F, a Loop6 Hinge Mutant of *Plasmodium falciparum* Triosephosphate Isomerase: Observation of an Intermediate Position of Loop6

K. Eaazhisai[1], H. Balaram[2], P. Balaram[1] and M. R. N. Murthy[1]*

[1]*Molecular Biophysics Unit Indian Institute of Science Bangalore, India*

[2]*Jawaharlal Nehru Centre for Advanced Science Research Jakkur, Bangalore, India*

**Corresponding author*

The enzymatic reaction of triosephosphate isomerase (TIM) is controlled by the movement of a loop (loop6, residues 166–176). Crystal structures of TIMs from a variety of sources have revealed that the loop6, which is in an open conformation in the unliganded enzyme, adopts a closed conformation in inhibitor complexes. In contrast, structures with loop open conformation are obtained in most of the complexes of TIM from the malarial parasite *Plasmodium falciparum* (PfTIM). W168 is a conserved N-terminal hinge residue, involved in different sets of interactions in the "open" and "closed" forms of loop6. The role of W168 in determining the loop conformation was examined by structural studies on the mutant W168F and its complexes with ligands. The three-dimensional structures of unliganded mutant (1.8 Å) and complexes with sulfate (2.8 Å) and glycerol-2-phosphate (G2P) (2.8 Å) have been determined. Loop6 was found disordered in these structures, reflecting the importance of W168 in stabilizing either the open or the closed states. Critical sequence differences between the *Plasmodium* enzyme and other TIMs may influence the equilibrium between the closed and open forms. Examination of the environment of the loop6 shows that its propensity for the open or the closed forms is influenced not only by Phe96 as suggested earlier, but also by Asn233, which occurs in the vicinity of the active site. This residue is Gly in the other TIM sequences and probably plays a crucial role in the mode of ligand binding, which in turn affects the loop opening/closing process in PfTIM.

Keywords: triosephosphate isomerase; *Plasmodium falciparum*; catalytic loop6; tryptophan mutant; flexibility

Introduction

The precise function of proteins is thought to involve intrinsic flexibility at the active site that allows different segments to move in relation to one another with relatively small energy cost.[1] Among these is often an active site loop, an open form of which facilitates binding and release of the ligand and a closed form which stabilizes, controls and protects the reaction intermediates.[2] Such a flexible loop has been extensively studied in triosephosphate isomerase (TIM).[1–11] Upon ligand binding, the atoms of this loop (loop6) were observed to move up to 8 Å, shielding the active site from solvent. The closed form is stabilized by a hydrogen bond between the loop and one of the terminal oxygen atoms of the phosphate group of the ligand. This active site loop motion has been shown to be the rate-limiting step of the reaction catalyzed by TIM;[10] the isomerization of dihydroxyacetone phosphate (DHAP) and glyceraldehyde-3-phosphate (GAP). Despite extensive data on the structural and kinetic properties of the catalytic loop of TIM, the factors that control its conformation are not fully clear. It is likely that the conserved N-terminal hinge residues (residues 166–168) or the residues at the tip of the loop (residues 169–173) or

Abbreviations used: TIM, triosephosphate isomerase; PfTIM, *Plasmodium falciparum* TIM; G2P, glycerol-2-phosphate; PGA, 2-phosphoglycolate; DHAP, dihydroxyacetone phosphate.

E-mail address of the corresponding author: mrn@mbu.iisc.ernet.in

the non-conserved C-terminal hinge residues (residues 174–176) or a combination of these controls the loop movement.

The propensity of the catalytic loop to adopt open or closed states seems to be very different in *Plasmodium falciparum* TIM (PfTIM), when compared to the other TIMs. Earlier studies of PfTIM[12–14] have shown that the loop6 predominantly occurs in the open conformation, in contrast to other TIMs where it closes on ligand binding when bound to ligands such as glycerol-3-phosphate (G3P),[15] 3-phosphoglycerate (3PG),[15] 2-phosphoglycolate (PGA)[16–20] and 2-phosphoglycerate (2PG).[21] Loop6 is also in an open conformation in the *Trypanosoma brucei* enzyme, where the active site has a bound *N*-hydroxy-4-phosphono-butanamide,[9] which has an additional methylene unit compared to the substrate. The unusual propensity of the catalytic loop of PfTIM to remain in the open state was attributed to the steric clash between Ile172 of loop6 and Phe96 (Ser in all the other TIMs). However, loop6 was found closed in the PfTIM-PGA complex, forcing Phe96 to take up an alternate conformation avoiding this steric clash.[13]

It is of interest to explore the possibility of the conserved N-terminal hinge residues being a determinant of the loop6 conformation. One of the N-terminal hinge residues of the catalytic loop6 is Trp168. PfTIM contains only two tryptophan residues, Trp168 and Trp11 (Figure 1(a)). Trp168 is a conserved residue, whereas Trp11 is found to be replaced by other aromatic residues in TIMs from various sources.[13] Trp11 is located in loop1 and is situated next to the catalytic residue Lys12. Two single tryptophan mutants of PfTIM, W168F and W11F, have been constructed to enable fluorescence studies to probe the loop dynamics.[6] A comparison of the fluorescence properties of native PfTIM with the mutant proteins, W11F and W168F, suggests that Trp168 shows unusual emission properties. This residue exhibits a high blue shifted emission (321 nm) and a significant red-edge excitation shift. Moreover, the fluorescence of Trp168 is substantially quenched. Also, this residue displays a significantly lower lifetime than Trp11. The k_{cat} value of the W168F mutant protein was almost twofold lower than that of the native enzyme. However, the K_m value for the mutant was comparable to the native PfTIM. The three-dimensional structure of PfTIM-2-phosphoglycerate complex, which has been solved to a high resolution (1.1 Å), clearly shows that the environment of Trp168 is highly polar and the residue is held tightly by a network of polar interactions with other residues in its vicinity. Examination of the interactions involving the N-terminal hinge residues (Figure 1(b) and (c)) shows that Pro166 is hydrogen bonded only to loop residues Trp168, Ala169 and Ile170 in the open form. The interaction with Ile170 is lost upon loop closure. Leu167 interacts with two residues from within the loop (Ala169 and Ile170) and two residues from outside the loop (Glu129 and Glu165). These interactions involve only main-chain atoms and are maintained upon loop closure. Of the three N-terminal hinge residues, only Trp168 is involved in protein–loop interactions that are different in the open and closed forms. The nitrogen atom of the indole ring of Trp168 is hydrogen bonded to OH of Tyr164 when the loop is in the open form. Upon loop closure, the indole makes a new hydrogen bond with OE2 of Glu129. Also, only in the open form, NE1 of Trp168 is hydrogen-bonded to NH1 of Arg134. Furthermore, one of the major conformational changes upon loop closure is in the χ^1 of Trp168, which changes by about 47°. Therefore, it is of interest to assess the influence of Trp168 on the structure and dynamics of the catalytic loop.

Here we further explore the structural features of loop6, based on additional structures: the structures of the W168F mutant of PfTIM and its complexes with sulfate and glycerol-2-phosphate (G2P; Figure 1(d)). The results are interpreted in terms of the sequence and structural similarities and differences of the residues in the vicinity of the active site between PfTIM and other TIMs. The results highlight the importance of Trp168 in the stabilization of specific loop conformation. A comparison of ligand-bound complexes of TIM provides further insight into the structural features that probably determine the loop orientation.

Results

The structures of W168F (1.8 Å), W168F-SO4 (2.8 Å), W168F-G2P (2.8 Å) and W11F-PGA (3.4 Å) have been determined with good stereochemical parameters (Table 1). In all the four cases, the asymmetric unit consists of a pair of dimeric molecules, permitting the observation of four independent subunits in each structure. The W11F-PGA crystals were of poor quality and diffracted only to 3.4 Å resolution. Nevertheless, in all the four independent subunits of W11F-PGA, electron density corresponding to loop6 (residues 166–176) revealed a closed conformation. The native PfTIM when complexed to PGA exhibits both open and closed conformations of the loop6.[13] Therefore occurrence of closed conformation in the W11F-PGA structure is not entirely surprising. As this structure was determined at a relatively low resolution of 3.4 Å, details of the structure have not been presented. The results and discussion are therefore based on the three W168F mutant structures.

Conformational state of loop6

Except for the loop6 residues, the overall structures of W168F, W168F-SO4 and W168F-G2P are identical. The root-mean-square (RMS) values for the equivalent C^α atoms (excluding the loop6 residues) of W168F/W168F-G2P, W168F/W168F-SO4 and W168F-G2P/W168F-SO4 are 0.26 Å, 0.23 Å and 0.22 Å, respectively. The conformations of the

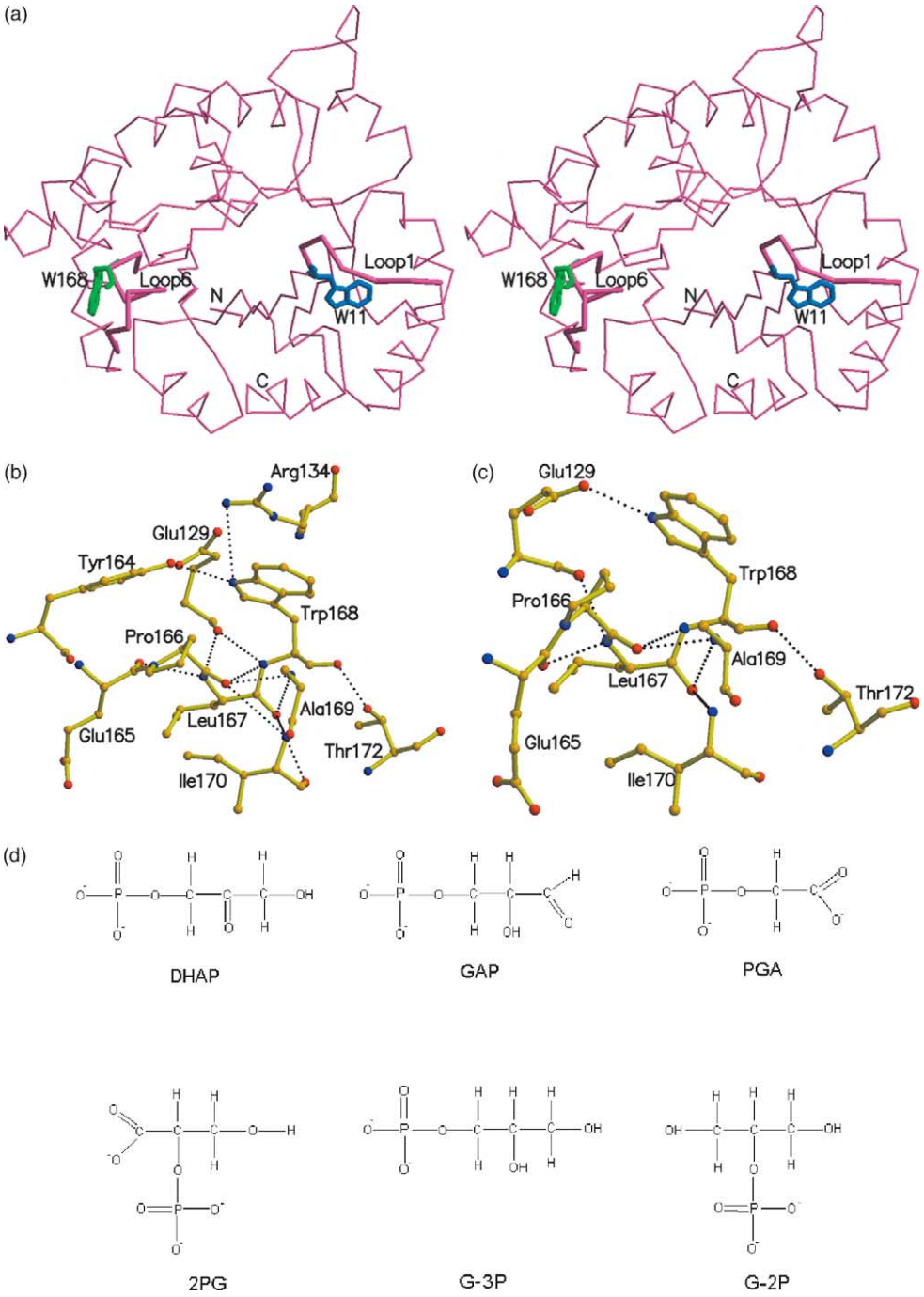

Figure 1. (a) Ribbon representation of the structure of PfTIM monomer. Trp11 (blue) and Trp168 (green) are shown in sticks. (b) and (c) Hydrogen bonding interactions of the N-terminal hinge residues, Pro166, Leu167 and Trp168 in the open and closed forms of loop6, respectively. The Figures were generated using MOLSCRIPT[39] and rendered using Raster3D.[40] (d) Chemical structures of the substrates and various ligands of TIM; dihydroxyacetone phosphate (DHAP), glyceraldehyde-3-phosphate (GAP), 2-phosphoglycolate (PGA), 2-phosphoglycerate (2PG), glycerol-3-phosphate (G-3P) and glycerol-2-phosphate (G-2P).

active site residues Lys12, His95 and Glu165 are similar in all the three structures.

In general, the electron density is not well defined for the loop6 residues (Figure 2(a)) in almost all the subunits of the three mutant structures. The loop6 is ordered in the A-subunit of unliganded W168F (Figure 2(b)), presumably because of the stabilization through crystal contacts. The residues at the tip of loop6, Gly171–Gly173 of the A-subunit, interact with residues 29–31 of the symmetry-related C-subunit through hydrogen bonding interactions involving main-chain atoms. The poorly defined loop6 residues of the other three subunits do not make crystal contacts. Nevertheless, in these subunits, electron density for the main-chain atoms of the N-terminal hinge residues 166 and 167 and

Table 1. Intensity data and refinement statistics of the solved structures

Parameters	W168F	W168F–SO4	W168F–G2P	W11F–PGA
A. *Intensity data statistics*				
Space group	$P2_1$	$P2_12_12_1$	$P2_12_12_1$	$P2_12_12_1$
Unit cell dimensions	a=53.7 Å b=106.2 Å c=89.5 Å β=92.4°	a=50.7 Å b=107.1 Å c=181.1 Å	a=51.1 Å b=108.5 Å c=178.8 Å	a=50.8 Å b=108.2 Å c=181.5 Å
Resolution (Å)	99.0–1.8	20.0–2.8	20.0–2.8	20.0–3.4
Number of unique reflections	93,113	25,154	25,351	15,710
Overall completion (%)	94.5 (89.0)	99.1 (98.6)	90.1 (85.5)	84.4 (49.1)
Multiplicity	2.4 (2.2)	3.3 (3.0)	3.0 (2.9)	4.4 (4.4)
I / σ(I)	15.2 (4.0)	5.8 (2.0)	3.2 (1.6)	6.9 (4.4)
Overall R_{merge} (%)	3.6 (21.4)	10.6 (31.9)	11.6 (36.8)	15.6 (27.7)
B. *Refinement statistics*				
Number of molecules/A.U.	2 dimers	2 dimers	2 dimers	2 dimers
Number of reflections				
(Working set)	81,661	20,988	15,270	10,813
(Test set)	5260	2362	1585	1247
R-factor (%)	20.7	18.1	21.9	22.4
R_{free} (%)	22.8	22.2	25.2	26.8
Number of protein atoms	7816	7800	7760	7816
Number of water molecules	558	148	142	34
Number of ligand atoms	–	20	40	36
RMS deviation				
Bond lengths (Å)	0.005	0.006	0.006	0.009
Bond angles (°)	1.25	1.23	1.24	1.41
Ramachandran statistics				
Most favored region (%)	93.3	92.4	91.7	85.4
Additional allowed region (%)	6.4	7.4	8.3	13.7
Generously allowed region (%)	0.3	0.2	0.0	0.9
Disallowed region (%)	0.0	0.0	0.0	0.0
B-average values (Å^2)				
Protein atoms	23.3	30.9	27.7	[a]
Ligand atoms	–	77.9	79.3	[a]
Water	20.4	30.8	26.4	[a]

Values in parenthesis refer to the highest resolution shell.
[a] B-factors (held unchanged) of the corresponding atoms of the refined structure of nativeTIM (PDB 1YDV) were used.

the C-terminal hinge residues (174–176) are well defined. Only a weak density is observed for the side-chain of Phe168. The residues at the tip of loop6 (residues 169–173) are completely disordered. The conformation of the hinge residues (Table 2) is similar to that of the open form of the loop. Similar features were observed for the loop6 residues of the other two complexes of W168F where loop6 is disordered in all the subunits.

Ligand binding at the active site

The structure of sulfate-bound W168F mutant was obtained in an attempt to determine the structure of the mutant complexed to the natural substrate DHAP. Instead of DHAP, a well-defined sulfate ion was found at the active site in all the four subunits of the mutant structure (Figure 3(a)). This structure is included for the analysis as sulfate is a competitive inhibitor of TIM.[22] The location of the sulfate ion at the active site is different from the corresponding position in the sulfate complexes of TrypTIM (PDB 5TIM) and *Caenorhabditis elegans* TIM (PDB 1MO0). After superposition of the subunits, the residual distances of the sulfate positions in TrypTIM and *C. elegans* TIM, from the corresponding position in the present complex, are 0.9 Å and 1.7 Å, respectively. Consequently, the protein–sulfate interactions in W168F-SO4 are different from the other two TIM sulfate complexes (Figure 3(b)). In the present case, O1 is hydrogen bonded to a water molecule (O–O distance 3.3 Å) and O2 is solvent-exposed. O3 is hydrogen bonded to OG of Ser211 (2.7 Å) and a water molecule (2.6 Å). As in phosphate-containing ligands, O4 of sulfate makes hydrogen bonds with N and ND2 of Asn233 (2.6 Å and 2.8 Å, respectively) and a water molecule (2.6 Å). As observed in other PfTIM complexes, where the ligands possess phosphate as anchoring group, Ser73 of the symmetry-related subunit makes water-mediated hydrogen bonding interactions with two of the oxygen atoms of the sulfate ion.

The active sites of all the four subunits in the structure of the W168F-G2P complex possess a bound G2P molecule. Figure 3(c) shows the fit of G2P to the F_o-F_c map obtained after omit refinement. The density for the ligand is much better defined in two (B and C) of the four subunits. This is consistent with the earlier observations on the asymmetry of ligand binding to PfTIM.[12–14] Figure 3(d) shows the protein–ligand hydrogen bonding interactions in the B-subunit. The interactions found in other subunits are very similar. The

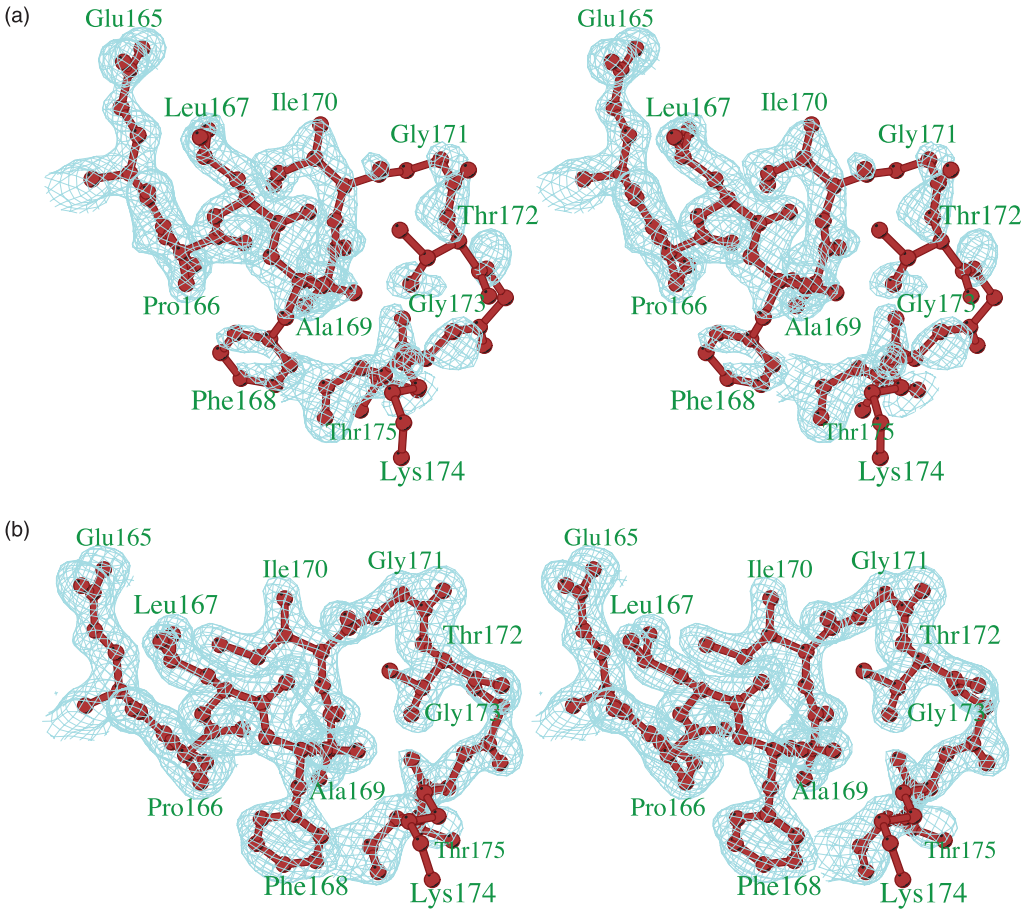

Figure 2. Stereo diagram illustrating the fit of the loop6 residues to the $2F_{obs}-F_{calc}$ electron density omit map contoured at 1.0σ. (a) Loop6 in the B-subunit is shown depicting the poorly defined electron density for the residues at the tip compared to the hinge residues. (b) Loop6 residues in the A-subunit of the unliganded W168F structure have well-defined density and are ordered. The Figures were prepared using the program BOBSCRIPT.[39]

phosphate moiety is anchored by the hydrogen bonding interactions between two of its oxygen atoms and OG of Ser211 (2.8 Å) and ND2 of Asn233 (2.8 Å), respectively. O2P is weakly hydrogen bonded to a water molecule (O–O distance 3.0 Å). This position of the phosphate moiety is ~2 Å away from the position observed in other TIMs and in PfTIM structures, where the loop6 is in the closed form. There is paucity of hydrogen bonds between the phosphate and various peptide NH groups in the present case (only two), when compared to the complexes of other TIMs[23] (seven or more). The O11 atom of the ligand is hydrogen bonded to NZ of Lys12 (2.80 Å). In this mode of binding, the O11 is fixed in a near-*cis* configuration with respect to the bridging oxygen atom O1P (O11-C1-C2-O1P ~ 0°). O31 atom is involved in three hydrogen bonding interactions; with the main-chain NH of Gly232 (O–N distance is 3.3 Å), the carbonyl oxygen atoms of Gly210 (O–O distance is 2.8 Å) and Leu230 (O–O distance is 2.6 Å). O31 interacts strongly with the residues 210–212, the conserved YGGS motif.

Conformational flexibility at the active site of PfTIM

The mode of binding of sulfate and G2P to the W168F mutant is different from that of the

Table 2. Ramachandran angles of the hinge residues of loop6

Residue number	Residue name	Phi in degrees		Psi in degrees	
		Open	Closed	Open	Closed
166	Pro	−80.7	−60.5	82.4	120.1
167	Leu	−61.0	−48.6	−29.5	−41.0
168	Trp	−60.0	−68.6	−18.2	−6.9
174	Lys	−91.9	−98.8	157.6	82.9
175	Thr	−131.2	−68.6	125.4	150.0
176	Ala	−85.9	−72.7	127.3	146.3

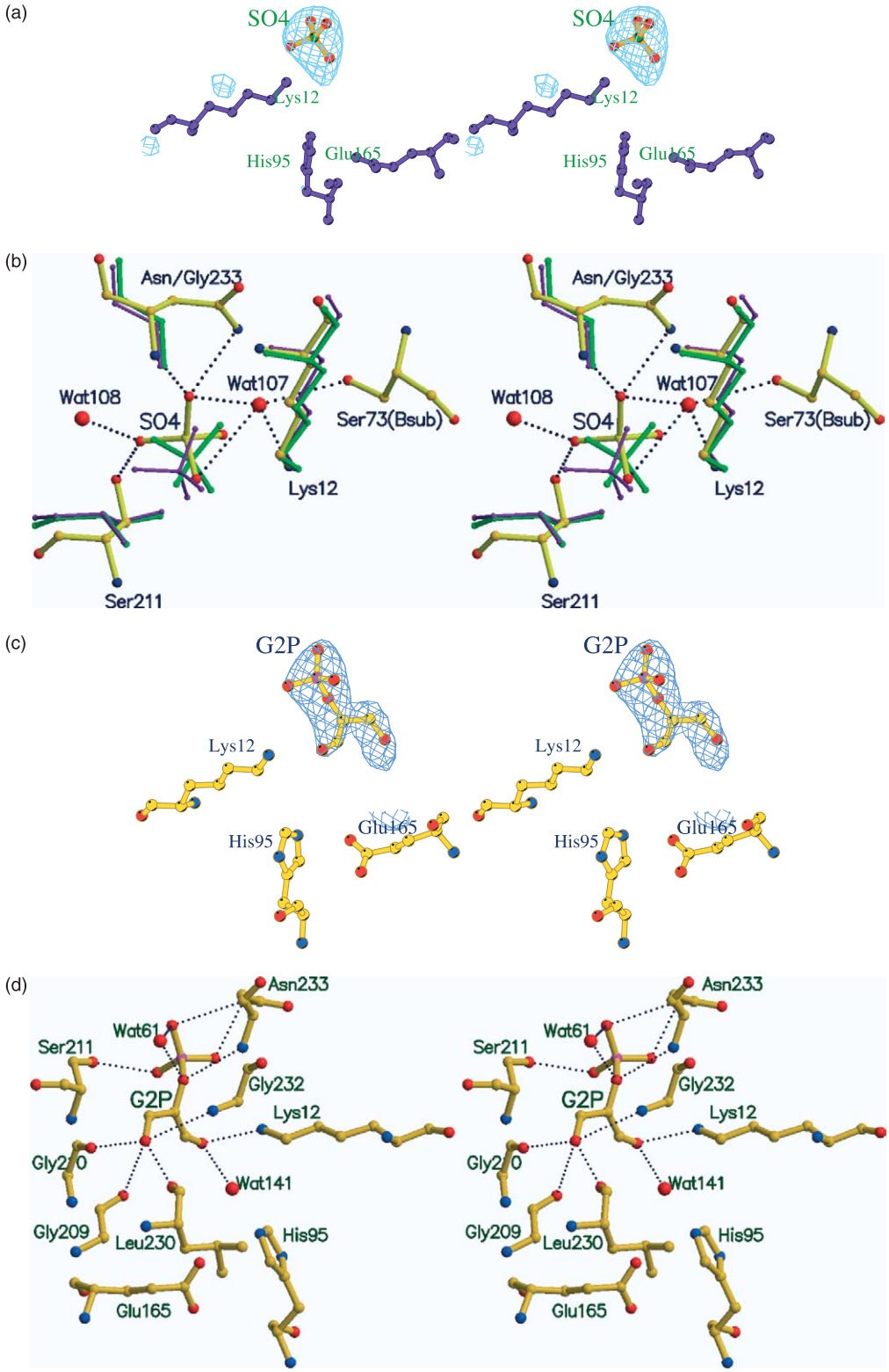

Figure 3. Stereo view of the ligand binding site in the structures of W168F mutant of PfTIM complexed with sulfate and G2P. (a) Fit of the sulfate ion to the electron density in a $F_{obs}-F_{calc}$ omit map contoured at 2.5σ. (b) Superposition of the active sites of sulfate complexes of TrypTIM (green), *C. elegans* TIM (indigo) and W168F mutant of PfTIM (colored by atom) showing the differences in the protein–ligand interactions. (c) G2P at the active site of the B-subunit of W168F–G2P complex is shown with density from the $F_{obs}-F_{calc}$ omit map contoured at 2.5σ. (d) Hydrogen bonding interactions (dotted lines) of G2P with the polypeptide.

complexes of other TIMs. Hence, it is worthwhile to examine the possible modes of ligand binding at the active site in all the PfTIM structures solved so far. These structures of PfTIM complexes can be classified as (a) ligand bound and loop open (open-loop structures) and (b) ligand bound and loop closed (closed-loop structures). Structural superposition suggests that there is a difference in the location of the phosphorus atom of the ligand with respect to the rest of the polypeptide between these two forms (Figure 4(a)). The phosphorus atom in all open-loop structures is 1–2 Å away from its position in the closed-loop structures. The observed location of the phosphorus atom in the G2P complex of W168F is consistent with that in the open form of the loop. However, there is only one mode of ligand binding in the structures of complexes of TIM from other sources. Plausible reasons for these differences were examined by a careful comparison of the active site geometries in the complexes of various TIMs. These studies indicated that the residues in the vicinity of the active sites are similar, except for the presence of Asn233 and Phe96 in PfTIM, which are Gly and Ser, respectively, in the other TIMs (Figure 4(b)). ND1 of Asn233 makes a strong hydrogen bond ($\leq$2.8 Å) with one of the phosphate terminal oxygen atoms of the ligand when the phosphorus atom is at the position corresponding to the loop-open form. This hydrogen bond becomes weaker ($\geq$3.5 Å) when the ligand is pushed to the position corresponding to the closed loop structures (Figure 4(c)).

In the ligand bound state, the catalytic acid, Glu165 of PfTIM, exhibits a distinct conformation when compared to the other TIMs. The side-chain of Glu165 in other TIMs undergoes a displacement such that its OE2 atom moves by 2.0–3.0 Å upon loop closure.[5] In PfTIM, this movement is limited to 1.0 Å. Residue 163, which interacts with the catalytic Glu165, is an Ala in all TIMs including PfTIM. However, this residue in the expressed mutant protein is a valine due to a cloning artifact. The CD atom of Glu165 in the open loop conformation (Figure 5) is at 3.7 Å from CG1 of Val163. In the closed loop structures, this distance is 3.0 Å. Placement of Glu165 in PfTIM at the position found in ligand-bound closed loop complexes of other TIM structures leads to a short contact with CG1 of Val163. In spite of the smaller movement in the side-chain of Glu165 (1.0 Å) in PfTIM, the hydrogen bonds involving the end of the ligand that corresponds to a potential reactive center in the substrate and the catalytic acid are retained. The various distances involving the three catalytic residues (Lys12, His95, and Glu165) and the ligand (PGA) are listed in Table 3 for PfTIM[13] and yeast TIM[24] complexed with PGA.

Discussion

TIM is one of the first enzymes in which occurrence of a large conformational change of a loop concurrently with catalysis was demonstrated. The current picture of the function of this loop in TIM is as a structured unit, that moves as a rigid body about its hinges, sequestering substrate from the solvent and selectively stabilizing the reactive intermediate in the isomerization reaction.[5,25] Mutagenesis experiments[5] have suggested that the stabilization of the closed loop is crucial for catalysis. In contrast, in PfTIM, the loop6 occurs more often in the open form and its dynamics appears to be significantly different from that in other TIMs. Therefore, the control of the loop movement in PfTIM is more difficult to decipher. The structures reported here were determined to examine the extent to which the conserved N-terminal hinge residues contribute to the preponderance of loop6 in the open form in PfTIM.

W168 is the only residue among the three N-terminal hinge residues that has unique interactions with respect to the open and closed forms of loop6. Thus, mutation of this residue may affect the stability of loop6. In the three W168F mutant structures reported here, loop6 has been observed in a disordered state in 11 independent subunits, emphasizing the importance of W168 in determining the loop orientation and/or integrity of the loop. In only one subunit (the A-subunit of unliganded W168F structure), loop6 is found to be ordered. Interestingly, the position of loop6 in this subunit is intermediate to the completely open and closed forms (Figure 6(a)). The C^{α} atom of Thr174, the residue at the tip of loop6, is 3.6 Å from that of the open form and 4.8 Å from that of the closed form. This suggests that this intermediate state of loop6 is closer to the open state. To characterize this conformation quantitatively, the distances between the C^{β} atoms of the loop residues and C^{β} atom of Ser211, which has been considered as a measure of the conformational state of the loop,[26] were estimated (Table 4). For Gly residues of the loop, C^{α} atoms were considered instead of C^{β}. Table 4 suggests that the loop6 in this subunit is indeed in an intermediate position with respect to the open and the closed forms. The Ramachandran angles of the intermediate form of loop6 in the mutant structure resemble those observed in the loop open form (Figure 6(b) and (c)). Large changes in ψ_{174} and ϕ_{175} corresponding to an approximately 80° tilt of the Lys174–Thr175 peptide bond occur with the loop closure, a feature noted in an earlier analysis.[25] This analysis also suggests that the loop6 moves as a "rigid body", with maximum conformational change at the hinges and minimum at the tip residues. Our results with the unliganded W168F mutant of PfTIM provide the first direct structure determination of loop6 in a position intermediate to the open and closed states, clearly supportive of the ideas of rigid body movement of loop6. Also, this observation provides structural support to McDermott's view that loop6 is dynamically active even in the absence of ligands.[7] Interestingly, a recent structural study on the unliganded rabbit muscle TIM[27] reveals that loop6

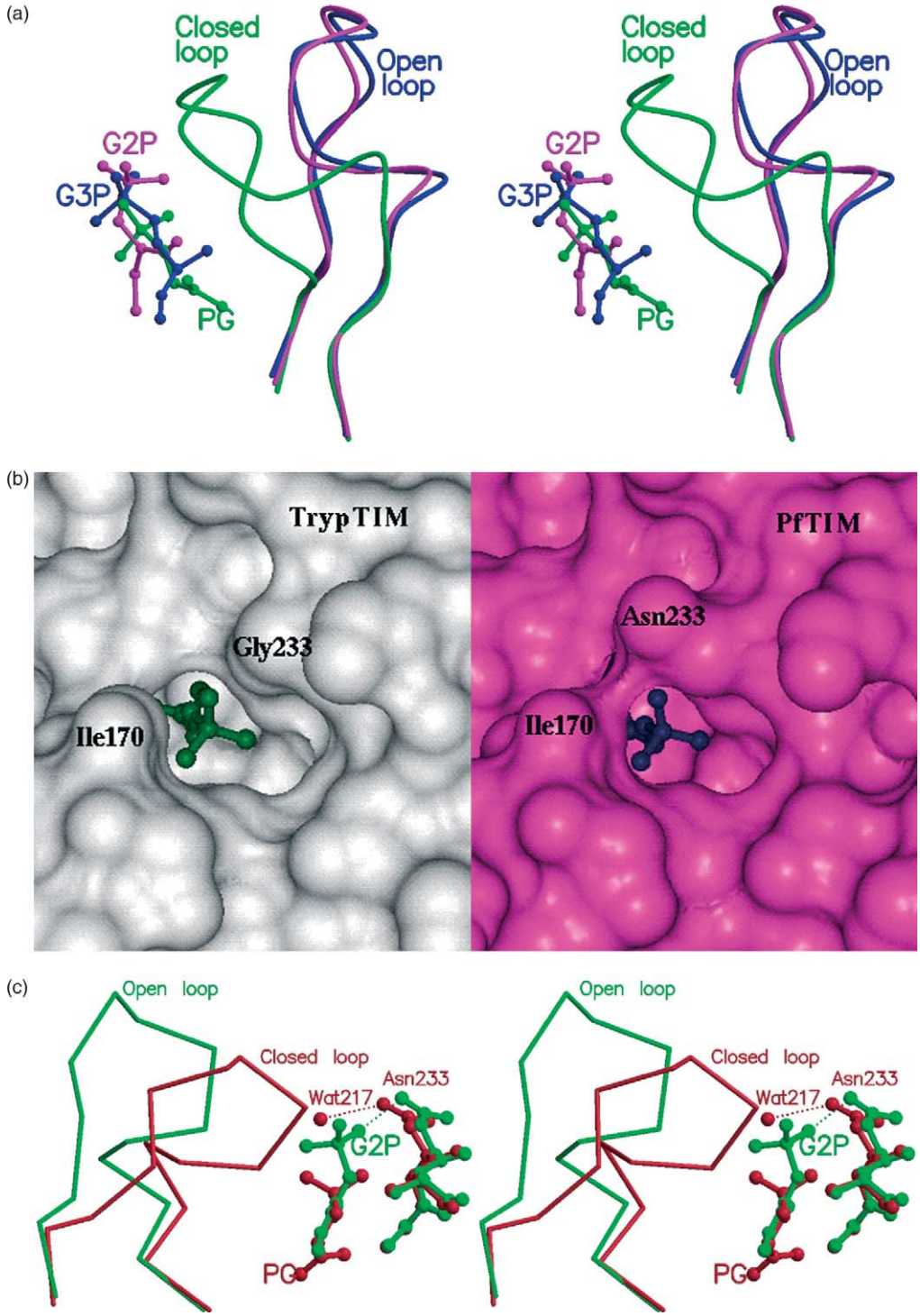

Figure 4. Illustrations of different modes of binding of the ligands to PfTIM. (a) Superposition of PfTIM-G3P (blue), PfTIM–G2P (magenta) complexes with the loop6 in the open form and PfTIM–PGA (green) complex in the closed form. (b) Space-filling models showing the residues in the vicinity of the binding sites of TrypTIM (white) and PfTIM (magenta). The ligand 2-phosphoglycolate is shown in ball-and-stick. The occurrence of Asn233 in PfTIM (Gly in TrypTIM) hinders the movement of the ligand deeper into the active site. This Figure was generated using INSIGHTII. (c) Stereo view of the interactions involving Asn233 and the ligand in the open (green) and closed (red) structures.

in one of the subunits adopts a closed conformation, while that in the other subunit is in the open form.

The observation of loop6 in a disordered state in most of the structures of unliganded and liganded W168F suggests that the stabilization of the local conformation of loop6 is drastically affected by the substitution of Trp by Phe. Both in the open and closed states, Trp168 is involved in hydrogen bonds that stabilize the loop6 conformation. In the open form of the wild-type enzyme, NE1 of Trp168 is 2.8 Å from the hydroxyl oxygen of Tyr164. In contrast, the tyrosine hydroxyl oxygen is 5.0 Å

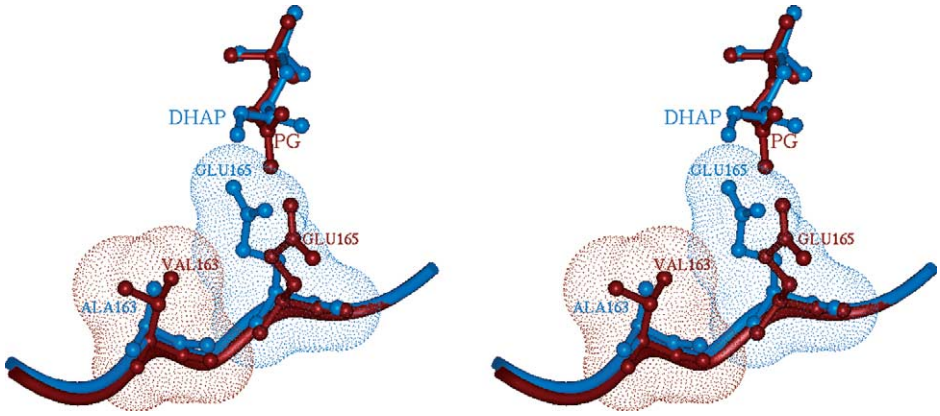

Figure 5. Stereo diagram showing the anticipated close steric contact between Val163 and Glu165 of PfTIM in the closed-loop conformation. The Figure was generated by the superposition of the closed-loop structures of YeastTIM–DHAP (blue; PDB 1NEY) and the PfTIM–PGA (red; PDB 1LYX) complexes. van der Waals surfaces for Val163, Glu165 (Pf and TrypTIMs) are shown.

away from the Trp168 NE1 atom in the closed structure. Nonetheless, in the closed form, a new hydrogen bond is formed between Trp168 NE1 and OE2 of Glu129 (2.7 Å). Removal of these potential hydrogen bonds together with the creation of a cavity due to the smaller volume of the Phe residue (135 $Å^3$) as compared to Trp (163 $Å^3$) is expected to destabilize the internal structure of the loop, which is consistent with the observation of lack of unique structure to the loop. Fluorescence experiments on the W11F mutant of PfTIM have suggested that Trp168 possesses unusual emission properties. It has been suggested that this unusual property may be due to its local electrostatic environment and its immobility.[6] The location of the phenyl ring of Phe168 in the mutant approximately coincides with that of the six-membered ring of the indole of Trp168 in the native structure. Also, the conformations of the residues that are in the vicinity of the site of mutation are largely similar. A comparison of the immediate environment of Trp168 in the 1.1 Å resolution structure of PfTIM–2PG complex[14] with that of Phe168 in the mutant suggests similar surroundings. The carboxylate of Glu129 forms hydrogen bonds with the phenolic hydroxyl of Tyr164 (2.62 Å) and the guanidino group of Arg134 (2.91 Å) in both the native and mutant structures. The plane of the guanidine group of Arg134 is parallel to the six-membered ring of Trp168 in the native structure and Phe168 in the mutant structure.

Examination of the ligand-binding mode in open and closed loop forms of PfTIM suggests that the loop closure might be coupled to the geometry of ligand binding in the Pf enzyme. In contrast to a unique mode in other TIMs, the ligands bind at different but distinct positions at the active site of PfTIM. Three different modes of ligand binding have been observed in the nine structures of PfTIM complexes determined so far[12–14] (and this paper). In the PfTIM–PGA complex, the phosphate moiety of the ligand is bound in a mode similar to that observed in TIM complexes from other sources. In this mode of ligand binding, the loop6 is closed. In the PfTIM–G3P complex, there is a difference of 1 Å in the location of the phosphorus atom from that in PfTIM–PGA complex. This mode corresponds to loop open form. In the W168F–G2P complex, the phosphate moiety of G2P occupies a position that is 2 Å away from that of PfTIM–PGA complex and the loop is disordered. These modes of ligand binding might be coupled to the loop motion. A steric clash between Phe96 and Ile170 has earlier been suggested as one of the reasons for the non-closure of loop6, despite ligand binding.[12–14] The present analysis shows that loop closure with the phosphorus atom at the position corresponding to the open-loop structure results in a steric clash (2.0 Å) between the main-chain oxygen of Gly171 and one of the phosphate oxygen atoms. Loop closure is therefore accompanied by the movement of the ligand deeper into the active site by 1–2 Å. This suggests that, apart from Phe96, the different modes of ligand binding could also be related to the different conformations of loop6. It is likely that these differences that are specific to PfTIM might be a result of the differences in the amino acid residues that interact with the ligand. A careful comparison of the ligand-binding site in various TIMs points to only one difference: Asn233 of PfTIM, which is Gly in all the other TIMs. Asn233 is located in loop8 and appears to be a flexible residue with a high *B*-factor in all the PfTIM structures. The occurrence of Asn233 at the active site appears to hinder the movement of the ligand to the site optimal for catalysis. Investigations on the site-specific mutants

Table 3. Hydrogen bond distances (Å) between the transition state analogue, 2-phosphoglycolate PGA and the catalytic residues of TIM

Hydrogen bond	PfTIM–PGA[13]	Yeast TIM–PGA[24]
Lys12 NZ···PGA O1	3.02	3.18
His95 NE2···PGA O1	2.69	2.89
Glu165 OE2···PGA O2	2.32	2.84

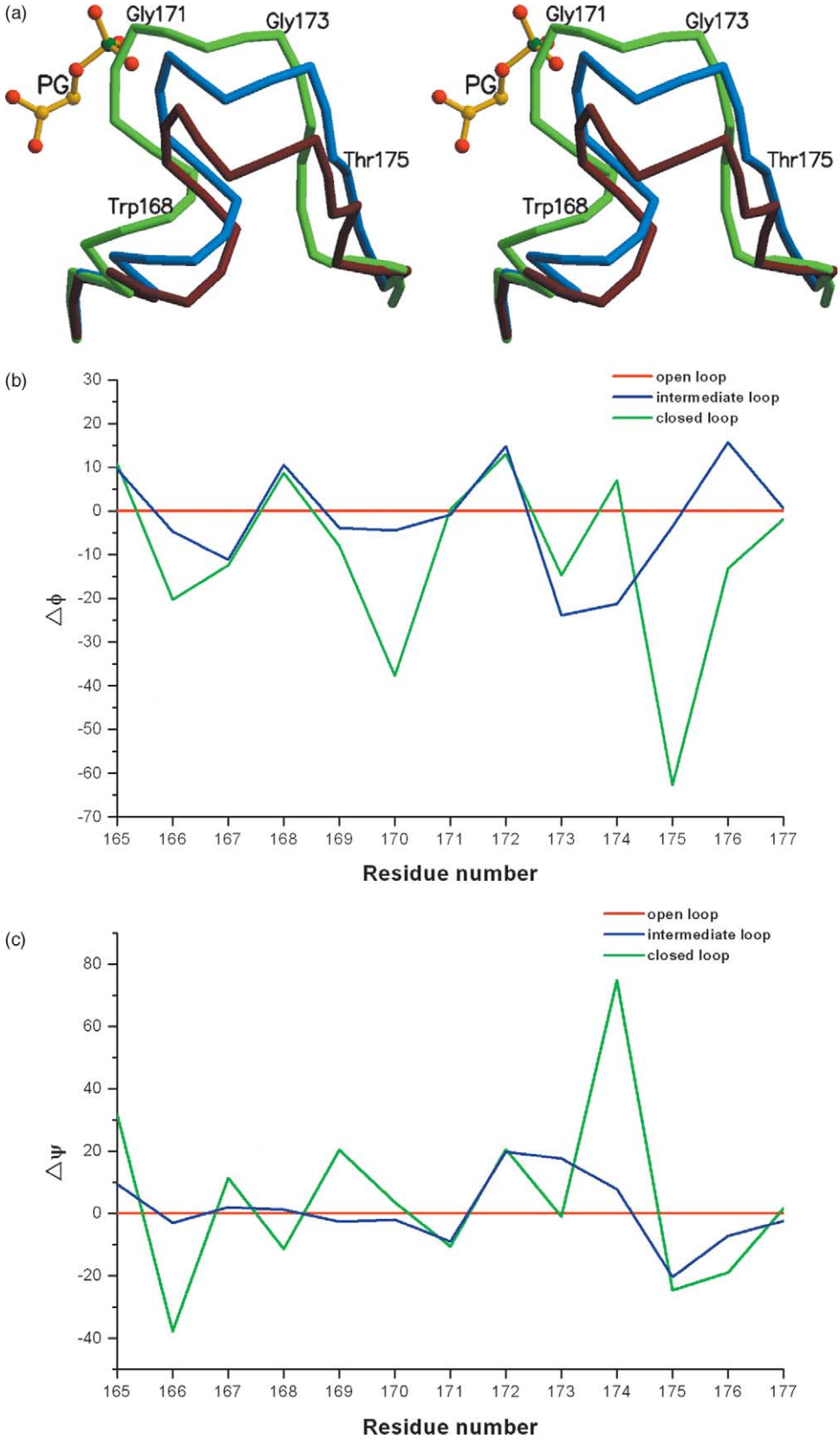

Figure 6. (a) Stereo view of the superposition of loop6 in the intermediate (blue), open (red) and closed (green) states of PfTIM structures. The structure of PfTIM–2PG complex (open loop) was used as the reference model on to which PfTIM–PGA (closed loop) complex and W168F-unliganded (intermediate) were superposed. (b) and (c) Plots showing the deviations in the Ramachandran angles, ϕ and ψ, respectively, of the residues of loop6 (166–176) in the intermediate and closed forms from those of the open form.

Table 4. Distances between C^{β} atoms of Ser211 and the loop6 residues

	Loop6 residues	TIM–2PG complex[14] (open loop)	TIM–PGA complex[13] (closed loop)	W168F (intermediate loop)
Ser211	Pro166	8.46	9.36	8.25
	Leu167	11.74	11.52	11.25
	Trp/Phe168	12.18	9.60	10.99
	Ala169	7.30	5.17	6.16
	Ile170	7.35	7.16	6.35
	Gly171	9.29	5.37	8.23
	Thr172	11.36	6.12	9.22
	Gly173	10.73	3.88	9.81
	Lys174	10.81	6.32	8.92
	Thr175	8.20	4.33	6.27
	Ala176	7.82	8.34	7.20

For Gly residues, C^{α} atoms are considered.

of this residue will further reveal the significance of Asn233 in PfTIM.

The coupling between loop closure and deprotonation of the ligand by Glu165 is believed to be a key feature in the mechanism of TIM catalysis.[5] Some flexibility is allowed in the positioning of Glu165 due to its location at the edge of a β-sheet, one residue before the "start" of the mobile loop.[5] In TIM complexes from other sources, the carboxylate of Glu165 is 2 Å closer to the C-1 and C-2 hydrogen atoms of the substrate in the closed structure when compared to the open form. In PfTIM, possibly because of a close steric contact between Val163 and Glu165, the side-chain movement is restricted to 1 Å. Occurrence of valine instead of alanine at position 163 is a cloning artifact in the expressed mutant protein. This artifact is common to the native PfTIM and its complexes, which include those with the loop6 in the open as well as the closed forms. This suggests that the artifact is unlikely to affect the conformation of the loop6. The smaller movement of Glu165 is coupled to loop closure as observed in PfTIM–PGA complex.[13] The ligand exhibits some additional flexibility, which allows its movement towards Glu165, thus reducing the distance between the carboxylate of Glu165 and C-1 and C-2 hydrogen atoms of the substrate to values found in other TIMs, thus enabling the proton transfer reaction. This suggests that the catalytic reaction in PfTIM is facilitated by structural plasticity at the active site with both protein and substrate movements being possible.

Conclusions

The crystal structure of the PfTIM mutant W168F and its complexes with sulfate and G2P were analyzed to elucidate the most probable factors driving the stability and conformation of loop6. The structures presented here revealed two findings. First, the stabilization of loop6 in PfTIM may be affected by perturbations in the N-terminal hinge residues, an observation consistent with their sequence conservation. In particular, Trp168 is important for anchoring the loop6 in either the open or closed forms. Substitution of this residue by Phe has resulted in a significant reduction in the k_{cat} value of about 40%.[6] However, W168F mutation, which has permitted the structural characterization of an intermediate loop6 position, does not interfere with ligand binding. The K_m of this mutant is comparable to that of the wild-type enzyme.[6] The unusual feature of the high propensity for open loop states of PfTIM appears to have no effect on the binding of ligands. Second, the conformation of loop6 in PfTIM is influenced by the sequence difference in the vicinity of the active site. In addition to Phe96 as suggested earlier,[13] the present structural study suggests Asn233, which interferes with the movement of the ligands/substrates into the active site, also as a critical residue in determining the loop6 conformation in PfTIM. Residues 96 and 233 are Ser and Gly, respectively, in all the TIM sequences determined so far except the *Plasmodium* species. Mutational analysis of these residues may provide further insights into the role of specific interactions in determining the relative stabilization and barrier for the interconversion between the open and closed forms of loop6 of PfTIM.

Materials and Methods

Purification

The recombinant mutant protein was expressed and purified as described earlier.[6] Briefly, the induced cells harboring the W168F plasmid were harvested and resuspended in 20 ml of 100 mM Tris–HCl (pH 8.0), 1 mM EDTA and lysed using a French press. The crude lysate was subjected to ammonium sulfate precipitation followed by an anion exchange chromatography using a 6 ml Resource-Q column. The protein was desalted by dialysis in a buffer containing 20 mM Tris–HCl (pH 8.0). The yield of the protein was measured spectrometrically using a molar extinction coefficient of $\varepsilon_{280} = 25{,}710\ M^{-1}\ cm^{-1}$. The protein was more than 95% pure as checked in 12% SDS-PAGE. The ligands used for the crystallization were purchased from SIGMA.

Crystallization

Both the mutant proteins, W11F and W168F, have been

crystallized at a concentration of 10 mg/ml. The complexes were prepared by incubating 10 mg/ml of the protein with the ligands in the molar ratio of 1 : 50 at 4 °C. Crystals of W168F and its complexes were grown in hanging-drops at 18 °C using standard vapor-diffusion techniques with the reservoir solution containing 20%–30% (v/v) PEG1450 (polyethylene glycol), 100 mM lithium sulfate and 100 mM sodium acetate (pH 4.5). While crystallizing W168F complexed with DHAP, care was taken to attenuate the enzyme reaction and phosphate elimination by performing crystallization and data collection at 4 °C. Crystals were obtained with the reservoir solution containing 20%–30% PEG1450, 10 mM lithium sulfate, 50 mM Tris (pH 8.0) and 5 mM DTT. However, it was found after determining the structure that only a sulfate was bound at the active site. Crystals of W11F–PGA complex were obtained using 20%–30% PEG1450, 100 mM lithium sulfate, 100 mM Tris (pH 8.0).

Data collection and processing

The data were collected on W168F and W168F-SO4 crystals at 100 K with 20% (v/v) glycerol as cryoprotectant, and on W11F-PGA and W168F-G2P crystals at room temperature using a MAR imaging plate detector system mounted on a Rigaku RU200 X-ray generator operating at 40 kV, 56 mA and equipped with a 200 μ focal cup. Data were processed using DENZO[28] and scaled using SCALEPACK.[28] The details of completeness and quality of the data are illustrated in Table 1.

Structure solution and refinement

The orientations and positions of the dimeric molecules in the unit cell were determined by molecular replacement technique using the program AMoRe[29,30] with the native TIM[31](PDB 1YDV) as the starting model. Residues were modeled using O and FRODO[32] into the electron density map obtained after extensive refinement and improved by iterative cycles of refinement using CNS.[33] Ligands and water molecules were built based on F_o-F_c and $2F_o-F_c$ maps. The geometrical parameters for the active site ligands in the complexes were obtained from HIC-UP.[34] Non-crystallographic symmetry (NCS) restraints were used only for the structures of the complexes. Individual atomic displacement parameters were refined for the protein, ligand and water atoms. To eliminate effects of phase bias from the starting model on the electron density calculated for the loop6 residues (166–178), both $2F_o-F_c$ and F_o-F_c omit maps were calculated with the entire stretch removed from the model in all the subunits of all the structures after applying simulated annealing. In the case of W168F mutant structures, examination of the $2F_o-F_c$ map at 1σ contour level and the F_o-F_c map at 2.5σ contour level showed density only for part of the hinge residues and not for the residues at the tip of the loop. Also solvent flattening did not improve the electron density in these regions of loop6. In W11F–PGA structure, $2F_o-F_c$ and F_o-F_c had better definition for the loop6 residues.

Sequence and structural analyses

The sequences of the TIMs used here were obtained from PUBMED, compiled from a variety of sources, including SwissProt, PIR, PRF, PDB, and translations from annotated coding regions in GenBank and RefSeq. Multiple sequence alignment was carried out using ClustalW program accepting the default parameters. The atomic coordinates were obtained from PDB. Structures of TIM from various sources possessing different conformations of loop6 were considered for the analysis. The structures chosen as representatives of the loop open and closed forms were the 1.1 Å structure of PfTIM complexed to 2PG[14] and 1.9 Å structure of PfTIM complexed to PGA,[13] respectively. The PDB codes of structures of other TIM complexes which have been determined to resolution better than 2.1 Å considered for the present study were as follows: 1IF2,[23] 1TPH,[35] 7TIM,[36] 1N55,[19] 1NEY[37] and PfTIM complexed to 2-phosphoglycolate (unpublished data). In these complexes, the loop6 has been observed in the closed form with a bound ligand at the active site. Structural superposition was done using the program ALIGN.[38] The graphical interpretations were done using the programs, O,[32] FRODO[32] and INSIGHTII.

Protein Data Bank accession numbers

The coordinates have been submitted to the RCSB Protein Data Bank. The PDB codes are 1VGA, 1WOA and 1WOB.

Acknowledgements

M.R.N.M. acknowledges the Council of Scientific and Industrial Research (CSIR), Government of India, Department of Science and Technology (DST) and the Department of Biotechnology (DBT) for financial support. P.B. acknowledges DST for financial support. Diffraction data on the mutants and complexes were collected using the X-ray facility for Structural Biology at the Molecular Biophysics Unit of the Indian Institute of Science supported by DST and DBT. Use of the facilities at the Supercomputer Education and Research Centre, Interactive Graphics Based Molecular Modeling Facility and the Bioinformatics Centre (supported by DBT) are acknowledged.

References

1. Xiang, J., Sun, J. & Sampson, N. S. (2001). The importance of hinge sequence for loop function and catalytic activity in the reaction catalyzed by triosephosphate isomerase. *J. Mol. Biol.* **307**, 1103–1112.
2. Desamero, R., Rozovsky, S., Zhadin, N., McDermott, A. & Callender, R. (2003). Active site loop motion in triosephosphate isomerase: T-jump relaxation spectroscopy of thermal activation. *Biochemistry*, **42**, 2941–2951.
3. Sun, J. & Sampson, N. S. (1999). Understanding protein lids: kinetic analysis of active hinge mutants in triosephosphate isomerase. *Biochemistry*, **38**, 11474–11481.
4. Pompliano, D. L., Peyman, A. & Knowles, J. R. (1990). Stabilization of a reaction intermediate as a catalytic device: definition of the functional role of the flexible loop in triosephosphate isomerase. *Biochemistry*, **29**, 3186–3194.
5. Sampson, N. S. & Knowles, J. R. (1992). Segmental movement: definition of the structural requirements for loop closure in catalysis by triosephosphate isomerase. *Biochemistry*, **31**, 8482–8487.

6. Pattanaik, P., Ravindra, G., Sengupta, C., Maithal, K., Balaram, P. & Balaram, H. (2003). Unusual fluorescence of W168 in *Plasmodium falciparum* triosephosphate isomerase, probed by single-tryptophan mutants. *Eur. J. Biochem.* **270**, 745–756.
7. Williams, J. C. & McDermott, A. E. (1995). Dynamics of the flexible loop of triosephosphate isomerase: the loop motion is not ligand gated. *Biochemistry*, **34**, 8309–8319.
8. Wierenga, R. K., Noble, M. E., Postma, J. P., Groendijk, H., Kalk, K. H., Hol, W. G. & Opperdoes, F. R. (1991). The crystal structure of the "open" and the "closed" conformation of the flexible loop of trypanosomal triosephosphate isomerase. *Proteins: Struct. Funct. Genet.* **10**, 33–49.
9. Verlinde, C. L., Witmans, C. J., Pijning, T., Kalk, K. H., Hol, W. G., Callens, M. & Opperdoes, F. R. (1992). Structure of the complex between trypanosomal triosephosphate isomerase and N-hydroxy-4-phosphono-butanamide: binding at the active site despite an "open" flexible loop conformation. *Protein Sci.* **1**, 1578–1584.
10. Rozovsky, S., Jogl, G., Tong, L. & McDermott, A. E. (2001). Solution-state NMR investigations of triosephosphate isomerase active site loop motion: ligand release in relation to active site loop dynamics. *J. Mol. Biol.* **310**, 271–280.
11. Sun, J. & Sampson, N. S. (1998). Determination of the amino acid requirements for a protein hinge in triosephosphate isomerase. *Protein Sci.* **7**, 1495–1505.
12. Parthasarathy, S., Balaram, H., Balaram, P. & Murthy, M. R. (2002). Structures of *Plasmodium falciparum* triosephosphate isomerase complexed to substrate analogues: observation of the catalytic loop in the open conformation in the ligand-bound state. *Acta Crystallog. sect. D*, **58**, 1992–2000.
13. Parthasarathy, S., Ravindra, G., Balaram, H., Balaram, P. & Murthy, M. R. (2002). Structure of the *Plasmodium falciparum* triosephosphate isomerase-phosphoglycolate complex in two crystal forms: characterization of catalytic loop open and closed conformations in the ligand-bound state. *Biochemistry*, **41**, 13178–13188.
14. Parthasarathy, S., Eaazhisai, K., Balaram, H., Balaram, P. & Murthy, M. R. (2003). Structure of *Plasmodium falciparum* TIM-2-phosphoglycerate complex at 1.1 Å resolution. *J. Biol. Chem.* **278**, 52461–52470.
15. Noble, M. E., Wierenga, R. K., Lambeir, A. M., Opperdoes, F. R., Thunnissen, A. M., Kalk, K. H. *et al*. (1991). The adaptability of the active site of trypanosomal triosephosphate isomerase as observed in the crystal structures of three different complexes. *Proteins: Struct. Funct. Genet.* **10**, 50–69.
16. Delboni, L. F., Mande, S. C., Rentier-Delrue, F., Mainfroid, V., Turley, S., Vellieux, F. M. *et al*. (1995). Crystal structure of recombinant triosephosphate isomerase from *Bacillus stearothermophilus*. An analysis of potential thermostability factors in six isomerases with known three-dimensional structures points to the importance of hydrophobic interactions. *Protein Sci.* **4**, 2594–2604.
17. Mande, S. C., Mainfroid, V., Kalk, K. H., Goraj, K., Martial, J. A. & Hol, W. G. (1994). Crystal structure of recombinant human triosephosphate isomerase at 2.8 Å resolution. Triosephosphate isomerase-related human genetic disorders and comparison with the trypanosomal enzyme. *Protein Sci.* **3**, 810–821.
18. Borchert, T. V., Kishan, K. V., Zeelen, J. P., Schliebs, W., Thanki, N., Abagyan, R. *et al*. (1995). Three new crystal structures of point mutation variants of monoTIM: conformational flexibility of loop-1, loop-4 and loop-8. *Structure*, **3**, 669–679.
19. Kursula, I. & Wierenga, R. K. (2003). Crystal structure of triosephosphate isomerase complexed with 2-phosphoglycolate at 0.83-Å resolution. *J. Biol. Chem.* **278**, 9544–9551.
20. Lolis, E. & Petsko, G. A. (1990). Crystallographic analysis of the complex between triosephosphate isomerase and 2-phosphoglycolate at 2.5-Å resolution: implications for catalysis. *Biochemistry*, **29**, 6619–6625.
21. Noble, M. E., Verlinde, C. L., Groendijk, H., Kalk, K. H., Wierenga, R. K. & Hol, W. G. (1991). Crystallographic and molecular modeling studies on trypanosomal triosephosphate isomerase: a critical assessment of the predicted and observed structures of the complex with 2-phosphoglycerate. *J. Med. Chem.* **34**, 2709–2718.
22. Hartman, F. C., LaMuraglia, G. M., Tomozawa, Y. & Wolfenden, R. (1975). The influence of pH on the interaction of inhibitors with triosephosphate isomerase and determination of the p*K*a of the active-site carboxyl group. *Biochemistry*, **14**, 5274–5279.
23. Kursula, I., Partanen, S., Lambeir, A. M., Antonov, D. M., Augustyns, K. & Wierenga, R. K. (2001). Structural determinants for ligand binding and catalysis of triosephosphate isomerase. *Eur. J. Biochem.* **268**, 5189–5196.
24. Lolis, E. & Petsko, G. A. (1990). Crystallographic analysis of the complex between triosephosphate isomerase and 2-phosphoglycolate at 2.5 Å resolution: implications for catalysis. *Biochemistry*, **29**, 6619–6625.
25. Joseph, D., Petsko, G. A. & Karplus, M. (1990). Anatomy of a conformational change: hinged "lid" motion of the triosephosphate isomerase loop. *Science*, **249**, 1425–1428.
26. Derreumaux, P. & Schlick, T. (1998). The loop opening/closing motion of the enzyme triosephosphate isomerase. *Biophys. J.* **74**, 72–81.
27. Aparicio, R., Ferreira, S. T. & Polikarpov, I. (2003). Closed conformation of the active site loop of rabbit muscle triosephosphate isomerase in the absence of substrate: evidence of conformational heterogeneity. *J. Mol. Biol.* **334**, 1023–1041.
28. Otwinowsky, Z. & Minor, W. (1997). Processing of X-ray diffraction data collected in oscillation mode. *Methods Enzymol.* **276**, 307–326.
29. Navaza, J. (1994). AMoRe: an automated package for molecular replacement. *Acta Crystallog. sect. A*, **50**, 157–163.
30. Navaza, J. & Saludjian, P. (1997). AMoRe: an automated molecular replacement program package. *Methods Enzymol.* **276**, 581–593.
31. Velanker, S. S., Ray, S. S., Gokhale, R. S., Suma, S., Balaram, H., Balaram, P. & Murthy, M. R. (1997). Triosephosphate isomerase from *Plasmodium falciparum*: the crystal structure provides insights into antimalarial drug design. *Structure*, **5**, 751–761.
32. Jones, T. A., Zou, J. Y., Cowan, S. W. & Kjeldgaard (1991). Improved methods for building protein models in electron density maps and the location of errors in these models. *Acta Crystallog. sect. A*, **47**, 110–119.
33. Brunger, A. T., Adams, P. D., Clore, G. M., DeLano, W. L., Gros, P., Grosse-Kunstleve, R. W. *et al*. (1998). Crystallography & NMR system: a new software suite for macromolecular structure determination. *Acta Crystallog. sect. D*, **54**, 905–921.

34. Kleywegt, G. J. & Jones, T. A. (1998). Databases in protein crystallography. *Acta Crystallog. sect. D*, **54**, 1119–1131.
35. Zhang, Z., Sugio, S., Komives, E. A., Liu, K. D., Knowles, J. R., Petsko, G. A. & Ringe, D. (1994). Crystal structure of recombinant chicken triosephosphate isomerase-phosphoglycolohydroxamate complex at 1.8-Å resolution. *Biochemistry*, **33**, 2830–2837.
36. Davenport, R. C., Bash, P. A., Seaton, B. A., Karplus, M., Petsko, G. A. & Ringe, D. (1991). Structure of the triosephosphate isomerase-phosphoglycolohydroxamate complex: an analogue of the intermediate on the reaction pathway. *Biochemistry*, **30**, 5821–5826.
37. Jogl, G., Rozovsky, S., McDermott, A. E. & Tong, L. (2003). Optimal alignment for enzymatic proton transfer: structure of the Michaelis complex of triosephosphate isomerase at 1.2-Å resolution. *Proc. Natl Acad. Sci. USA*, **100**, 50–55.
38. Cohen, G. E. (1997). ALIGN: a program to superimpose protein coordinates accounting for insertions and deletions. *J. Appl. Crystallog.* **30**, 1160–1161.
39. Kraulis, P. J. (1991). MOLSCRIPT: a program to produce both detailed and schematic plots of protein structures. *J. Appl. Crystallog.* **24**, 946–950.
40. Merritt, E. A. & Bacon, D. J. (1997). Raster3D: photorealistic molecular graphics. *Methods Enzymol.* **277**, 505–524.

Edited by I. Wilson

(Received 23 May 2004; received in revised form 12 August 2004; accepted 13 August 2004)